Tunneling recombination mechanism in n-type a-Si:H steady state regime

Tobbeche Souad[*a] and Merazga Amar[b]

[a]Laboratoire des matériaux semi-conducteurs et métalliques, Faculté des Sciences et de la

Technologie, Département de Génie-Electrique, Université de Biskra,

B.P. 145, Biskra 07000, Algérie.

[b]Physic Department, Faculty of Sciences, King Khaled University,

PO Box 3236, Abha, Saudi Arabia.

[a]souad_tobbeche@yahoo.fr, [b]Merazga_amar@yahoo.fr

Keywords: DOS – a-Si:H – steady state photoconductivity – tunneling – recombination.

Abstract. In this paper we developed a recombination model for the steady state photoconductivity (SSP) with the assumption that the correlated dangling bond states (DB) act as the essential recombination centres and the electron recombination proceeds by tunneling from the conduction band tail states (TS) for n-type a-Si:H. The modeled temperature dependence of the SSP presents the main measured features, particularly the small activation energy and the thermal quenching.

Introduction

A characteristic feature of hydrogenated amorphous silicon (a-Si:H) is the disorder-induced localisation of states near the band edges which leads to mobility edges and to tails of localised states extending deep into the gap. In addition, a fairly large number of deeper dangling bond states is expected to exist, which originate from defects in the amorphous network or impurities. The properties of a-Si:H depend sensitively on the density and energy distribution of these localised gap states. In particular, these states determine the transport and the recombination in this semiconductor.

In the steady state regime, the recombination mechanism involving carrier tunneling from tail states (TS) to DB states was first detected by Dersch et al [1] from the spin dependent photoconductivity technique. This was later modeled by Cleve et al [2] using exponential band TS and a single level of DB recombination centres. Satisfactory values for the activation energy and the thermal quenching of the photoconductivity were obtained. Zhou et al [3] modeled the recombination which takes place by direct tunneling between electrons and holes trapped in the band tails. It was shown that this model could account for all the general features exhibited by the photoconductivity of a-Si:H in the low-temperature region, although the magnitude of the photoconductivity predicted by the model tended to be larger than that measured.

An analytical study of the transient photoconductivity (TPC) in the pre-recombination time range, based on a multiple trapping (MT) model which takes into account the thermal equilibrium distribution, was applied to TPC data measured in lightly Phosphorous doped a-Si:H. This allowed to determine the density of shallow localised states of the CBT and indicated a sharp drop near 0.17 eV below the mobility edge for this data [4].

In this paper we develop a recombination model for the SSP which uses this part of the conduction band tail in the density of states (DOS), with the assumption that the correlated DB states act as the essential recombination centres and the electron recombination proceeds by tunneling from the conduction band tail states. Hole tunneling transitions to DB states were ignored since these would not modify the SSP for n-type material. It will be shown that the modeled temperature and excitation dependences of the SSP present the main features encountered in the literature [5-7], particularly the thermal quenching and the low activation energy.

Steady state photoconductivity

Density of states

For an n-type a-Si:H, the portion of the conduction band tail around the level E_t is determined by the pre-recombination TPC [4]. The distribution around E_t can be approximated by:

$$g_c(E) = G_c.\exp\left(\frac{E}{k.T_{c1}}\right).\left[1 - \frac{1}{1+\exp\frac{E-E_t}{k.T_{c0}}}\right] \qquad (1)$$

Where the tail characteristic temperature changes from T_{c1}, for $E<E_t$, to $T_{c1}.T_{c0}/(T_{c1}+T_{c0})$ for $E>E_t$. The DOS at E_c is $G_c=1.5\times10^{21}$ cm^{-3}.eV^{-1} as found in the literature. E_t is fixed at level -0.17 eV [4]. The tail characteristic temperatures T_{c1} and T_{c0} are 650 K and 160 K respectively. The DOS distribution around E_t is shown in Fig. 1 where the characteristic temperature falls to $(T_{c1}.T_{c0})/(T_{c1}+T_{c0})=128$ K below E_t.
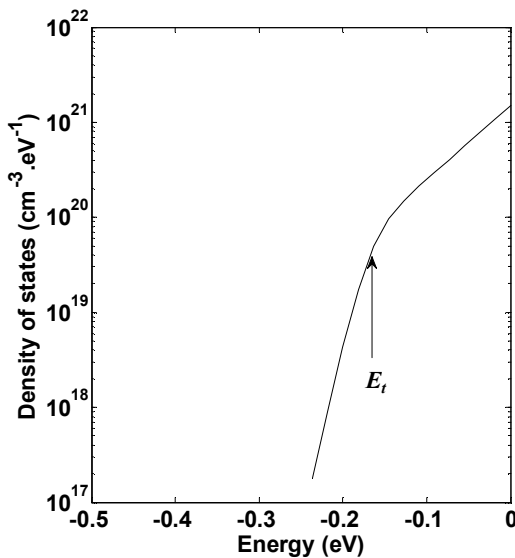

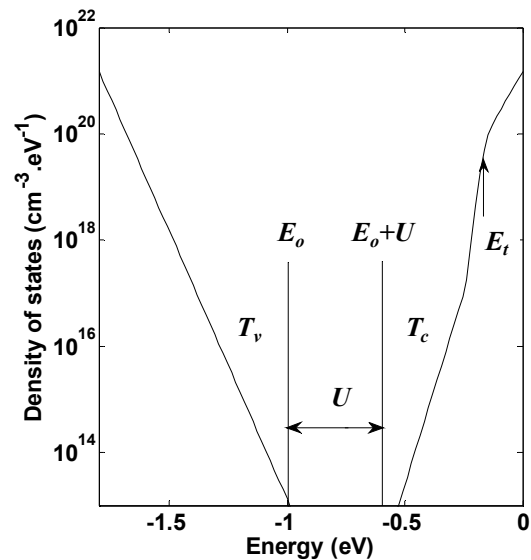**Fig. 1** The conduction band tail profile.

Fig. 2 Density of states used in the model.

The DOS distribution used in the model is shown in Fig. 2. In addition to the portion of the conduction band tail around E_t determined by the pre-recombination TPC, the model DOS contains exponential band tails with $T_c=350$ K and $T_v=500$ K. Discrete levels $E_0=E_v+0.8$ eV and E_o+U are assigned to D^+/D^o and D^-/D^o DB states respectively, with $U=0.4$ eV denoting the correlation energy.

Recombination model

The model is based on two assumptions: The dominance of DB states as recombination centres and the processing of electron recombination through tunneling from tail states. Fig. 3 shows the transitions involved in the recombination process in steady state conditions. Since the hole contribution to SSP is negligible in n-type material, we include only free holes in the capture transitions. Two additional assumptions are made:
The probability of free electron capture by DB states is negligible compared to tunneling probability ($C_{nt}^o.n_t \gg C_n^o.n$) and the tail states intervening in the tunneling process are predominantly located around E_t where the tail falls sharply and the excess charge peaks.

Considering the transitions in Fig. 3,

Fig. 3 Recombination transition rates with the indexes meaning: *cn*: electron capture, *en*: electron emission, *cnt*: electron capture from TS, *cp*: hole capture, *ep*: hole emission, o: from or to D^o, -: from or to D^-, +: from or to D^+.

the rate equations at different transition levels are:

At E_t:
$$\frac{dn_t}{dt} = 0 = C_n.(N_t - n_t).n - C_n.N_c.\exp\left(\frac{E_t}{k.T}\right).n_t + C_{nt}^+.n_{t1}^+.N.F^o$$
$$+ C_{nt}^o.n_{t1}^o.N.F^- - C_{nt}^+.n_t.N.F^+ - C_{nt}^o.n_t.N.F^o \tag{3}$$

At $E_o + U$:
$$\frac{dF^-}{dt} = 0 = C_{nt}^o.n_t.F^o - \left(C_{nt}^o.n_{t1}^o + C_n^o.n_1^o\right).F^- + C_p^-.p_1^-.F^o - C_p^-.p.F^- \tag{4}$$

At E_o:
$$\frac{dF^+}{dt} = 0 = -C_{nt}^+.n_t.F^+ + \left(C_{nt}^+.n_{t1}^+ + C_n^+.n_1^+\right).F^o - C_p^o.p_1^o.F^+ + C_p^o.p.F^o \tag{5}$$

F^o, F^- and F^+ are the occupation fractions of the D^o, D^- and D^+ states respectively, and N the total density of DB states such that

$$N.\left(F^o + F^+ + F^-\right) = N \tag{6}$$

n, p, n_t are respectively the free electron, the free hole and the trapped (at E_t) electron densities. $N_c = k.T.G_c$, $N_v = k.T.G_v$ and $N_t = k.T.g(E_t)$ are the effective DOS at E_c, E_v and E_t. C_n^o, C_n^+, C_p^o and C_p^- are the capture coefficients of a free electron by D^o, a free electron by D^+, a free hole by D^o and a free hole by D^- respectively. C_{nt}^o and C_{nt}^+ are the capture coefficients of trapped electrons by D^o and D^+ respectively. n_1^o and n_1^+ are the electron emission densities to extended states from D^- and D^o respectively, obtained by detailed balance consideration [8] with the degeneracy factors 1/2 and 2:

$$n_1^o = 2N_c \exp\left(\frac{E_o + U}{k.T}\right) \text{ and } n_1^+ = \frac{1}{2}N_c \exp\left(\frac{E_o}{k.T}\right) \tag{7}$$

p_1^o and p_1^- are the hole emission densities from D^+ and D^o:

$$p_1^o = 2N_v \exp\left(\frac{E_v - E_o}{k.T}\right) \text{ and } p_1^- = \frac{1}{2}N_v \exp\left(\frac{E_v - U - E_o}{k.T}\right) \tag{8}$$

We define analogously n_{t1}^o and n_{t1}^+ as electron emission densities from D^- and D^o to tail states at E_t.

$$n_{t1}^o = 2N_t \exp\left(\frac{E_o + U - E_t}{k.T}\right) \text{ and } n_{t1}^+ = \frac{1}{2}N_t \exp\left(\frac{E_o - E_t}{k.T}\right) \tag{9}$$

The addition member to member of eq. (2) and eq. (3) gives

$$G = \underbrace{\left[n_t.c_{nt}^+.N.F^+ - N_1^+.N.F^o\right]}_{R_{n1}} + \underbrace{\left[n_t.c_{nt}^o.N.F^o - N_1^o.N.F^-\right]}_{R_{n2}} \tag{10}$$

Where $N_1^+ = C_n^+.n_1^+ + C_{nt}^+.n_{t1}^+$ and $N_1^o = C_n^o.n_1^o + C_{nt}^o.n_{t1}^o$ the total probability of electron emission to extended and localised states from D^o and D^- states respectively, $N^+ = n_t.C_{nt}^+ + p_1^-.C_p^o$ the probability of the transfer D^+ to D^o, $P^o = p.C_p^o + N_1^+$ the probability of the transfer D^o to D^+, $P^- = p.C_p^- + N_1^o$ the probability of the transfer D^- to D^o and $N^o = n_t.C_{nt}^o + p_1^-.C_p^-$ the probability of the transfer D^o to D^-. Two dependent recombination paths can then be defined: path1 involving the reversible transfer D^+ to D^o with recombination rate R_{n1} and path2 involving the reversible transfer D^o to D^- with recombination rate R_{n2}. The occupation fraction F^o of the D^o states is obtained from eqs. (4), (5) and (6) as

$$F^o = \frac{N^+.P^-}{(N^+.P^- + P^o.P^- + N^o.N^+)} \tag{11}$$

In terms of excess charge density, the charge neutrality equation can be written

$$(p - p_o) + dQ_v + N.\left(F^+ - F_o^+\right) - (n - n_o) - dQ_c - N.\left(F^- - F_o^-\right) = 0 \tag{12}$$

Where F_o^+ and F_o^- are the thermal equilibrium D^+ and D^- occupancies [9], n_o and p_o are the thermal equilibrium free carrier concentrations calculated using the charge neutrality equation

$$p_o - n_o - Q_c(n_o, p_o) + Q_v(n_o, p_o) - N.\left(F_o^- - F_o^+\right) + N_d = 0 \tag{13}$$

and $dQ_{c,v}(n, p) = \int_{C,V} g_{c,v}(E).\left[f_{SRH}(E) - f_{FD}(E)\right].dE$ are the excess trapped charge densities in the conduction (c) and valence (v) band tails with f_{SRH} and f_{FD} the appropriate steady state Schokley-Read-Hall and equilibrium Fermi-Dirac functions. N_d stands for the ionized doping donors density. To calculate the SSP given by

$$\sigma_{ph} = q.\left[\mu_n.n + \mu_p.p\right] \tag{14}$$

One has to solve numerically the system of eqs. (2), (10) and (12) for n, p and n_t. However, in this particular case of n-type material, F^+ is much less than F^o and F^- so that eq. (11) can be reduced to $F^o = P^-/(P^- + N^o)$. Consequently, the predominant recombination path is path2 and eq. (10) reduces to

$$G = R_{n1} = n_t.C_{nt}^o.N.F^o - N_1^o.N.F^-. \tag{15}$$

With these further simplifications, a quadratic equation of variable n_t, and n-dependent coefficients is easily derived from eqs. (2) and (15)

$$A(n).n_t^2 + B(n).n_t + C(n) = 0 \tag{16}$$

The charge neutrality equation is then solved using a simple bissection method. The parameter values used in the solution are: To prevent recombination to tail states in the model, the trapping coefficients are such that for the conduction band tail $C_p=0$ and $C_n=10^{-9}$ cm^3.s^{-1}, and for the valence band tail $C_n=0$ and $C_p=10^{-9}$cm^3.s^{-1} [10]. The donors and dangling bonds densities are $N_d=N=10^{16}$ cm^{-3}, giving an average position of the dark Fermi level at 0.5 eV below E_c. The free carrier capture coefficients to DB states are $C_n^+ = C_p^- = 10^{-7}$ cm^{3}s^{-1} and $C_n^o = C_p^o = 10^{-9}$ cm^{3}s^{-1} while the localised electron capture coefficients are $C_{nt}^+ = C_n^+/100$ and $C_{nt}^o = C_n^o/100$ [2]. The free electron and hole nobilities are $\mu_n = 10$ and $\mu_p = 0.3$ cm^{2}V^{-1}s^{-1} [11].

Results and discussions

Fig. 4 shows the modeled temperature dependence of the SSP for six different excitation intensities G over a range extending from 100 to 450 K. All the features experimentally observed [5-7] are reproduced: Region (I) with a small activation energy ($E_p \sim 0.09$ eV) appearing at low or intermediate temperatures depending on the excitation level G, Region (II) around a maximum at T_M which shifts towards high temperatures with increasing G and Region (III) around a minimum at T_m which also shifts towards high temperatures when G increases. For $T > T_m$ σ_{ph} increases more rapidly.
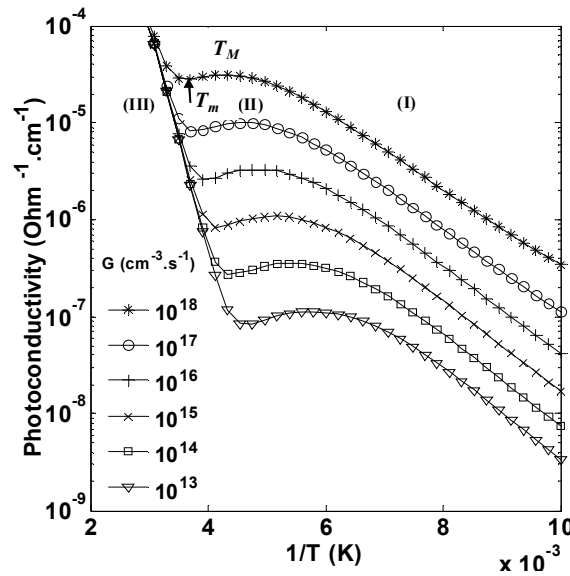

Fig. 4 Temperature dependence of SSP for six different excitation G.

In order to interpret these results, we examine the influence of the simultaneous variations, in each temperature region, of the different gap charge densities which intervene in the charge neutrality equation on the variation of the free electron density n [12]. We chose $G=10^{17}$cm^{-3}s^{-1} for the temperature dependence (Fig. 5) and $T=150$ K for the excitation dependence (Fig. 6).

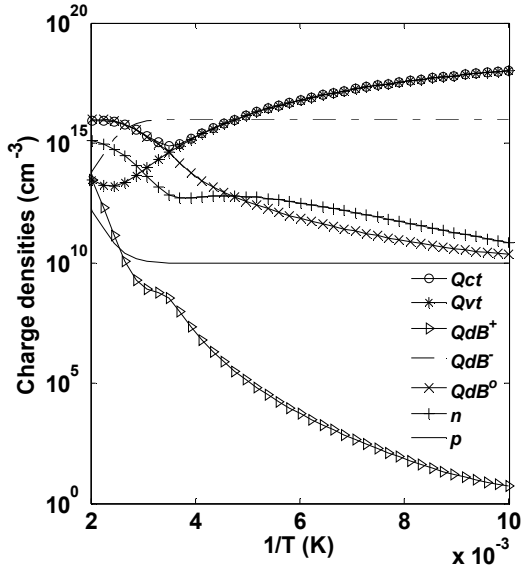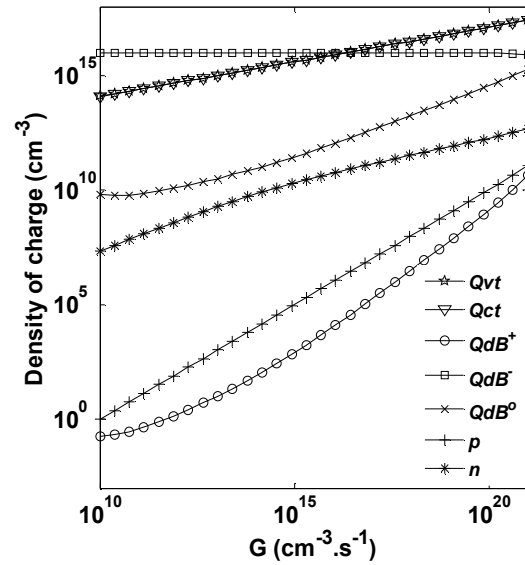**Fig. 5** Temperature dependence of the different charge densities for $G=10^{17}$ cm^{-3}.s^{-1}.

Fig. 6 Excitation dependence of charge densities for T=150 K.

Region (I): The band tail charges Q_c and Q_v predominate the charge neutrality and superimpose each other (Fig. 5).

$$Q_c(1/T)=Q_v(1/T) \tag{17}$$

Adopting zero temperature statistics, in the case of a single conduction band tail characteristic temperature T_c below E_t, Q_c and Q_v can be approximated by

$$Q_c \approx \int_{E_v}^{E_{fn}} g_c(E).dE \approx k.T_c.G_t.\exp\left(\frac{-E_t}{k.T_c}\right).\left(\frac{n}{N_c}\right)^{\alpha_c} \tag{18}$$

$$Q_v \approx \int_{E_{fp}}^{E_c} g_v(E).dE \approx k.T_v.G_v.\left(\frac{p}{N_v}\right)^{\alpha_v} \tag{19}$$

Where $g_c(E) = G_c \exp\left(\frac{E-E_t}{kT_c}\right)$ and $g_v(E) = G_v \exp\left(\frac{E_v - E}{kT_v}\right)$ are the conduction and valence band tail states densities. $G_t = g_c(E_t)$, $\alpha_c = T/T_c$ and $\alpha_v = T/T_v$. The hole density p is constant in the temperature range of region (I). Fig. 6 shows that Q_{dB}^-, the D$^-$ charge density is constant and p varies linearly with G over the whole excitation range. Therefore, we can conclude that the hole recombination via D$^-$ states is monomolecular and p is given by

$$p = G.\tau_p \tag{20}$$

With τ_p the hole life time which can be determined from Fig. 6 in two different ways: Using eq. (20) with $p = 10^{10}$ cm^{-3} and $G = 10^{17}$ cm^{-3}.s^{-1}, so $\tau_p = 10^{-7}$ s and using $\tau_p = 1/(c_p^-.N)$ with $Q_{dB}^- = 10^{16}$ cm^{-3}, so $\tau_p = 10^{-7}$ s. This value of τ_p is close to that determined by Spear et al using the

drift mobility technique [13]. Eqs. (18) and (19) lead to the following SSP expression as a function of T and G.

$$\sigma_{ph} \approx q.\mu_n.n = q.\mu_n.N_c.\exp\left(\frac{E_t}{k.T}\right).(x)^{T_c/T}.\left(\frac{G.\tau_p}{N_v}\right)^{T_c/T_v} \tag{21}$$

Where $x = \left(\frac{T_v}{T_c}\right).\left(\frac{G_v}{G_t}\right)$ is a constant relating the band tails parameters.

The activation energy E_p and the power index γ of the SSP are respectively

$$E_p = k.\frac{d\log(\sigma_{ph})}{d(1/T)} = E_t + k.T_c.\log(x)$$

and $\gamma = \dfrac{d\log\sigma_{ph}}{d\log G} = \dfrac{T_c}{T_v}$

If we take for T_c the main value of 350 K (for $E < 0.25$ eV) and 128 K (for $E > 0.25$ eV), we will obtain $E_p \approx$ -0.08 eV which is very close to 0.09 eV determined from the slope of region (I). The drop of γ to values less than 0.5 at high excitations [14] is readily explained by the decrease of T_c as the quasi-Fermi level moves towards E_c.

Region (II): in region (I) the charge neutrality is controlled by the band tails and the recombination process is determined by hole capture by the D^- states. This increases Q_{dB}^o as the D^- states convert into D^o. In region (II) Q_{dB}^o increases more rapidly with temperature, leading to the curvature of n (or σ_{ph}) towards a maximum at T_M followed by a decrease with increasing T (Thermal quenching).

Region (III): This region is characterized by a pronounced increase of n (or σ_{ph}) starting from a minimum at T_m. This results from the decrease of Q_{dB}^- through electron emission [12]. The hole lifetime τ_p increases and p must also increase. The increase of Q_{dB}^o is a direct result of D^- to D^o conversion while the increase of Q_c is a consequence of E_{fn} shift following the increase of n. Q_v continues decreasing since the hole quasi Fermi level is still shifting towards E_v with increasing temperature despite the increase of p.

In Fig. 7, we plot the energy distribution of the electron charge Q_c at $G=10^{17}$ cm^{-3}s^{-1} for many different temperatures.

It can be seen that the charge peak is situated around E_t, especially at low temperatures, which would mean that the tunneling probability $C_{nt}^+.n_t$ is maximal at E_t. We plot in Fig. 8, as a function of temperature, n_t as calculated from the model statistics, and the charge peak density $f_{SRH}(E_t).g(E_t).dE$. Almost a total superimposition of the two curves is observed, which clearly justifies the assumption of considering E_t as a representative discrete level in the tunneling recombination process.
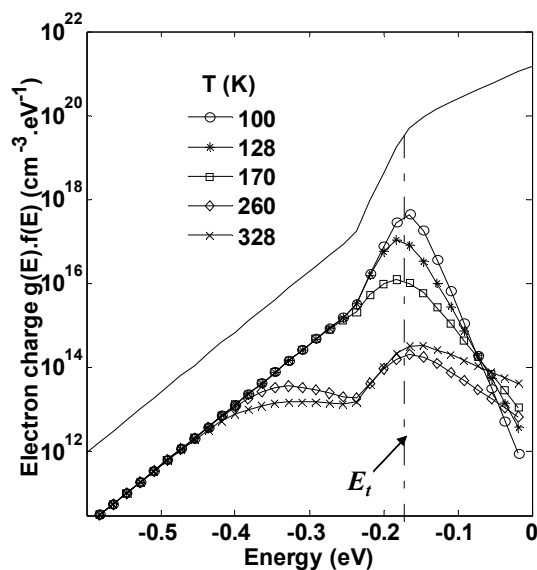
Fig. 7 Energy distribution of the electron charge $g(E).f(E)$ for five temperatures under excitation $G=10^{17}cm^{-3}.s^{-1}$.
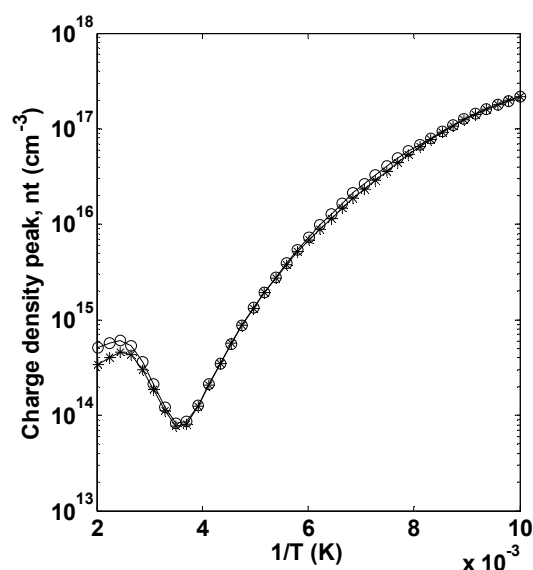
Fig. 8 Electron concentration n_t ($-*-$), the charge peak $f(E_t).g(E_t).dE$ ($-o-$) as function of $1/T$ for $G=10^{17}cm^{-3}.s^{-1}$.

Conclusion

In conclusion we have presented a recombination model for the steady state photoconductivity in n-type a-Si:H, in which the main recombination centres are correlated dangling bonds and the electron recombination occurs indirectly, through tunneling from shallow localised states. The model calculations are remarkably simplified using a single discret level for these intermediate states. This approximation is applicable when a particular DOS with a sharp drop around this level is used such as the case of lightly Phosphorous doped a-Si:H from analysis of the pre-recombination TPC data. Some of the SSP features are related to the DOS parameters, namely the relatively low temperature activation energy, the thermal quenching and the power index of the excitation dependence.

References

[1] H. Dersch, L. Schweitzer, J. Stuke, Phys. Rev. B 28 (1983) 4678.
[2] B. Cleve, P. Thomas, in: amorphous silicon technology materials research, society symposium proceedings, San Francisco (1990) 317.
[3] J. H. Zhou, S. R. Elliott, Phys. Rev. B 48 (1993) 1505.
[4] A. Merazga, H. Belgacem, C. Main, S. Reynolds, Solid State Comms. 112 (1999)535.
[5] J. K. Yoon, J. Jang, C. Lee, J. Appl. Phys 64 (1988) 6951.
[6] M. Q. Tran, Phil. Mag. B 72 (1995) 35.
[7] K. Shimakawa, Ashtosh Ganjoo, Phys. Rev. B 65 (2002) 165213.
[8] J. G. Simmons, G. W. Taylor, Phys. Rev. B 4 (1971) 502.
[9] H. Okamoto, H. Kida, Y. Hamakawa, Phil. Mag. B 49 (1984) 231.
[10] C. Main, J. Berkin, A. Merazga,in:New Physical Problems in Electronic Materials, ed. M. Borissov, N. Kirov, J. M. Marshall and A. Vavrek (world scientific, Singapore,1991) 55.
[11] W. E. Spear, S. C. Cloude, Phil. Mag. Lett. 55 (1987) 271.
[12] T. Smail, T. Mohammed-Brahim, Phil. Mag B 64 (1991) 675.
[13] W. E. Spear, H. L. Steemers, P.G. LeComber, R. A. Gibson, Phil. Mag. B 50 (1984) L33.
[14] M. Hack, S. Guha, M. Shur, Phys. Rev. B 30 (1984) 6991.

Advanced Technologies in Manufacturing, Engineering and Materials
10.4028/www.scientific.net/AMR.774-776

Tunneling Recombination Mechanism in n-Type a-Si:H Steady State Regime
10.4028/www.scientific.net/AMR.774-776.816

DOI References

[1] H. Dersch, L. Schweitzer, J. Stuke, Phys. Rev. B 28 (1983) 4678.
http://dx.doi.org/10.1103/PhysRevB.28.4678

[3] J. H. Zhou, S. R. Elliott, Phys. Rev. B 48 (1993) 1505.
http://dx.doi.org/10.1103/PhysRevB.48.1505

[4] A. Merazga, H. Belgacem, C. Main, S. Reynolds, Solid State Comms. 112 (1999)535.
http://dx.doi.org/10.1016/S0038-1098(99)00408-1

[6] M. Q. Tran, Phil. Mag. B 72 (1995) 35.
http://dx.doi.org/10.1080/13642819508239062

[7] K. Shimakawa, Ashtosh Ganjoo, Phys. Rev. B 65 (2002) 165213.
http://dx.doi.org/10.1103/PhysRevB.65.165213

[8] J. G. Simmons, G. W. Taylor, Phys. Rev. B 4 (1971) 502.
http://dx.doi.org/10.1103/PhysRevB.4.502

[9] H. Okamoto, H. Kida, Y. Hamakawa, Phil. Mag. B 49 (1984) 231.
http://dx.doi.org/10.1080/13642817408246510

[11] W. E. Spear, S. C. Cloude, Phil. Mag. Lett. 55 (1987) 271.
http://dx.doi.org/10.1080/09500838708214696

[12] T. Smail, T. Mohammed-Brahim, Phil. Mag B 64 (1991) 675.
http://dx.doi.org/10.1080/13642819108207629

[14] M. Hack, S. Guha, M. Shur, Phys. Rev. B 30 (1984) 6991.
http://dx.doi.org/10.1103/PhysRevB.30.6991